Vol 18 No 2, February 2009
1674-1056/2009/18(02)/0531-06

Chinese Physics B

© 2009 Chin. Phys. Soc.
and IOP Publishing Ltd

Helium production from ^{84}Kr– and ^{197}Au–emulsion interactions at high energies*

Zhang Dong-Hai(张东海)†, Cheng Jin-Xia(程锦霞), Cheng Bin(成 宾), Wang Fang(王 芳), Wang Qi(王 琦), Zhang Hai-Qing(张海青), Xu Rong(许 蓉), Jia Hui-Ming(贾会明), and Li Xue-Qin(李雪琴)

Institute of Modern Physics, Shanxi Normal University, Linfen 041004, *China*

(Received 6 March 2008; revised manuscript received 24 June 2008)

The properties of the relativistic helium fragments produced in interactions of ^{84}Kr at 1.8 A GeV and ^{197}Au at 10.7 A GeV in emulsion are investigated. The experimental results are compared with those obtained from various projectiles with emulsion collisions at different energies. It is found that the multiplicity distribution of helium projectile fragments (HPFs) is well described by the Koba–Nielsen–Olesen (KNO) scaling presentation. The second Mueller moment f_2 of the HPF multiplicity distribution is independent of the projectile energy for the same projectile, but it is dependent on the projectile mass number. The value of f_2 increases with the increase of projectile mass number A_p. The negative value of f_2, when $A_p < 69$, means that the emission of HPFs is anticorrelated, but positive value of f_2, when $A_p > 69$, refers to that the emission of HPFs is correlated. The non-zero f_2 moment in this experiment implies the strong correlation existing between the HPFs.

Keywords: relativistic heavy-ion collisions, projectile fragmentation, nuclear emulsion
PACC: 2570N, 2587, 2940R

1. Introduction

The multiplicity distribution of the produced fragments has been regarded as a potentially useful source of information of the production mechanism. The production of helium projectile fragments (HPFs) in relativistic nucleus–nucleus collisions has been studied extensively.[1−19] It is found that the multiplicity distribution of HPFs can be well represented by the Koba–Nielsen–Olesen (KNO) scaling hypothesis,[20] and the production rate of HPFs is independent of the beam energy, but it increases with the increase of projectile mass. The angular distribution or transverse momentum distribution of HPFs from heavy projectile has a long tail which cannot be explained by using a single Gaussian distribution. These distributions imply the existence of two distinct sources of HPFs. The dominant one is the cold source with an average excitation energy of about 7–10 MeV and the other is assumed to be of a fireball type at a high temperature of 40–70 MeV.[9,10,21]

Sengupta *et al* [5] have studied the dependence of average HPF multiplicity $\langle n_\alpha \rangle$ on the mass number of projectile A_p by using the data from ^{16}O–, ^{32}S–, ^{56}Fe–, and ^{84}Kr–emulsion interactions and found that the experimental data can be approximately parametrized by the relation $\langle n_\alpha \rangle = aA^b$ with a=0.48, b=0.41, and χ^2/DOF=0.04, where DOF stands for Degree of Freedom. El-Nadi *et al* [13] have made the same investigation by using the data from ^{12}C-, ^{22}Ne-, ^{24}Mg-, and ^{28}Si–emulsion interactions and found that the best fitting parameters are a=0.79± 0.28, b=0.25±0.09 and χ^2/DOF=0.35. Recently Jilany[3] also has studied the same dependence by using the data from ^{12}C–, ^{16}O–, ^{22}Ne–, ^{24}Mg–, ^{28}Si–, ^{32}S–, ^{197}Au–, and ^{208}Pb–emulsion interactions, and different fitting parameters (a=0.37±0.02, b=0.47±0.01) are observed. So it seems that the dependence of $\langle n_\alpha \rangle$ on A_p is closely related to the data set used.

Mueller[22] has shown that the binomial moment f_2 of multiplicity distribution is useful for describing and analysing the multiparticle final state. A non-zero f_2 moment implies the presence of strong cor-

*Project supported by the National Natural Science Foundation of China (Grant Nos 10475054 and 10675077), the Foundation for Key Program of Ministry of Education of China (Grant No 2 05026), the Natural Science Foundation of Shanxi Province, China (Grant No 200801105) and the Shanxi Provincial Foundation for Returned Scholars, China.
†Corresponding author. E-mail: zhangdh@dns.sxnu.edu.cn

relation between the HPFs. Sengupta *et al* [5] first discussed the second Mueller moment of HPFs produced in ultra-relativistic heavy ion collisions. Recently Jilany[3] has given a compiler of the second Mueller moment of multiplicity distribution of HPFs from different projectiles at high energies. In both papers positive values of f_2 are given. If we follow the formula given by Mueller to recalculate the values of f_2, it is found that the values of f_2 are negative, apart from the values for Kr, Au, and Pb–emulsion interactions.

In the present paper we carry out a detailed investigation of HPF distribution of 1.8 A GeV ^{84}Kr– and 10.7 A GeV ^{197}Au–emulsion interactions, including the HPF multiplicity distribution and the dependence of average multiplicity $\langle n_\alpha \rangle$ on the projectile mass number. Considering the correlation of multiparticle final state, we systematically collect the data of HPF production, recalculate the second Mueller moment, and give a detailed study of the correlation between the second Mueller moment f_2 of HPFs multiplicity distribution and the projectile mass number for the first time for relativistic nucleus–nucleus interactions. It is found that the second Mueller moment increases linearly with the projectile mass number increasing from negative value for small projectile to positive value for heavy projectile.

2. Experimental details

Two stacks of nuclear emulsion pellicles of $10\times10\times0.06\,\mathrm{cm}^3$ in volume, provided by EMU-01 Collaboration, were used in this experiment. One stack of Ilford G-5 emulsion was exposed horizontally to ^{84}Kr beam at an energy of 1.8 A GeV at the Bevatron at Lawrence Berkeley Radiation Laboratory (LBL). Another stack of NIKFI BR-2 emulsion was exposed horizontally to 10.6 A GeV ^{197}Au ions at the Brookhaven Alternating Gradient Synchrotron (AGS). The density of the beam was about 10^3 nuclei/cm^2. Interactions were found by along-the-track scanning technique with an oil immersion objective of 100×magnification. The beam tracks were picked up at 5 mm away from the edge of the plate and carefully followed until they either interacted with emulsion nuclei or escaped from any surface of the emulsion.

A total of 477 and 1787 inelastic events produced in ^{84}Kr– and ^{197}Au–emulsion interactions were located respectively. Out of them, 392 and 1614 events having at least one HPF are investigated respectively in the present work. For each interaction, the number of shower particles (n_s) corresponding to single charged relativistic secondaries with speed $\beta \geq 0.7$ and ionization less than 1.4 times the plateau ionization for single charged minimum ionizing particles is determined. These particles mainly consist of produced π-mesons and singly charged fragments. The number of slow-moving ($\beta < 0.7$) heavily ionizing particles, n_h, is also determined. Their corresponding tracks are classified into (i) grey tracks n_g ($0.3 \leqq \beta < 0.7$ and range in emulsion $R > 3\,\mathrm{mm}$), which consist of tracks arising from the recoiled protons with kinetic energy E_k=40–400 MeV and (ii) tracks from low-energy fragments that are emitted from the excited target nucleus known as black tracks n_b and are single and multicharged fragments with $E_k < 40$ A MeV, $\beta < 0.3$ and range $R < 3\,\mathrm{mm}$. The heavy track multiplicity, n_h, is shown to be equal to $n_g + n_b$, i.e. $n_h = n_g + n_b$.

At relativistic energies, multiply charged fragments with charge $Z \geq 2$, emitted from the breakup of the projectile, essentially travel at the same speed as that of the beam. These energetic projectile fragments are recorded in emulsion with a 100% detection efficiency. In general, the detection of HPFs is quite definite due to their distinctive grain density in nuclear emulsion. HPFs that are emitted in the forward cone with respect to the beam direction have grain density $g_\alpha \approx 4g_{\min}$ (where $g_{\min}$ is the grain density of the minimum ionizing particles and it is about 12 and 30 grains/100 micron for ^{84}Kr– and ^{197}Au–emulsion interactions respectively) and not changed within 2 cm away from its production point.

3. Experimental results

Figure 1 presents the normalized HPF multiplicity distribution with ^{84}Kr and ^{197}Au projectiles, which is obtained in the present work. For comparison the results obtained from ^{16}O, ^{24}Mg, ^{28}Si, ^{32}S, and ^{208}Pb projectiles with emulsion interactions at different energies are also included in the figure. It can be seen that the multiplicity distribution of HPFs becomes broader with the increase of the projectile mass number. This broadening is physically expected since the number of participant helium clusters becomes larger for larger projectiles.

The validity of the KNO[20] scaling of the HPFs produced in heavy-ion interactions at high energies

has been confirmed by many experimental groups. The KNO scaling hypothesis was originally derived by assuming the Feynman scaling of the inclusive particle production cross section. According to the KNO scale, the HPF multiplicity distribution p(n_α) in high energy collisions obeys the scaling law

$$\psi(Z) = 4Z\exp(-2Z), \tag{1}$$

where

$$\psi(Z) = \langle n_\alpha\rangle p(n_\alpha) = \langle n_\alpha\rangle \sigma_{n\alpha}/\sigma_{\rm nuc}. \tag{2}$$

$\psi(Z)$ should be an energy-independent function of the scaled variable $Z = n_\alpha/\langle n_\alpha\rangle$, where n_α represents the number of HPFs produced in an event and $\langle n_\alpha\rangle$ is the average HPF multiplicity of the whole data sample. $\sigma_{\rm nuc}$ refers to the total inelastic cross-section and $\sigma_{n\alpha}$ is the partial cross-section for the reaction channel with multiplicity n_α.

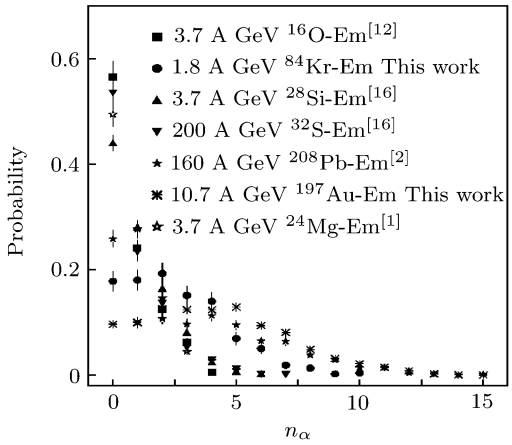


Fig.1. The normalized multiplicity distributions of HPFs of different projectiles with emulsion interactions at various incident energies.

In Fig.2 we plot $\langle n_\alpha\rangle p(n_\alpha)$ as a function of the scaled variable $n_\alpha/\langle n_\alpha\rangle$ for HPFs produced in ^{84}Kr– and ^{197}Au–emulsion interactions at 1.8 A GeV and 10.7 A GeV respectively. The experimental data are fitted by relation $\psi(Z) = AZ\exp(-BZ)$. The fitting parameters A and B are 3.95±0.17 and 2.17±0.03, respectively, and χ^2/DOF is 0.20. These values are reasonably close to the values of A and B compiled in Ref.[8] and the theoretical values of A=4 and B=2.

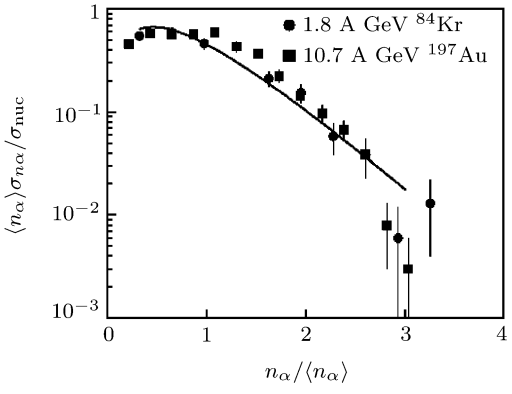


Fig.2. The multiplicity distribution $\langle n_\alpha\rangle\sigma_{n\alpha}/\sigma_{\rm nuc}$ versus $n_\alpha/\langle n_\alpha\rangle$ for HPFs.

The energy independence of multiplicity scaling can also be studied by using C_q moment given by

$$C_q = \langle n_\alpha^q\rangle/\langle n_\alpha\rangle^q = \langle Z^q\rangle = \int Z^q\psi(Z){\rm d}Z. \tag{3}$$

Table 1 presents the experimental results of the average multiplicity and the C_q ($= \langle n_\alpha^q\rangle/\langle n_\alpha\rangle^q$) moment of the HPFs from our ^{84}Kr– and ^{197}Au–emulsion interactions. For comparison, our previous results from ^{16}O–emulsion interactions at 3.7 and 60 A GeV and results from interactions of ^{12}C, ^{16}O, ^{20}Ne, ^{24}Mg, ^{28}Si, ^{32}S, ^{40}Ar, ^{56}Fe, ^{197}Au and ^{208}Pb with emulsion at the different incident energies are also included, showing that the C_2 moment does not change with the energy and the mass number of projectile, but the higher moments show the indication of a slow increase with the projectile mass number.

To further study the dependence of average HPF multiplicity $\langle n_\alpha\rangle$ on the mass number of projectile A_p, we have collected as many as possible data of HPF production in high-energy nucleus–nucleus interactions as listed in Table 1. Figure 3 shows that the value of $\langle n_\alpha\rangle$ varies with A_p and that the experimental data can be approximately parametrized by the formula

$$\langle n_\alpha\rangle = k_1 A_p^{k2}, \tag{4}$$

where k_1=1.327±0.027 and k_2=0.017±0.001 with χ^2/DOF=0.672. But in the result obtained from Ref.[4] by using the projectile mass $A_p \le 32$, k_1= 1.108±0.369, and k_2=0.146±0.116 are used. The

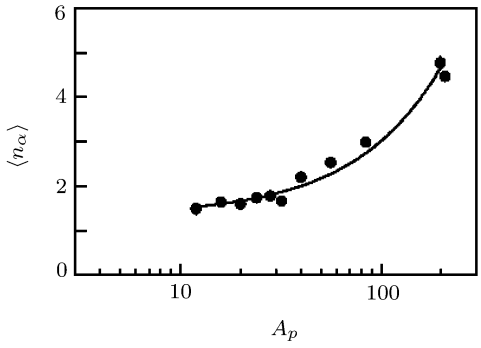


Fig.3. The average HPF multiplicity $\langle n_\alpha\rangle$ versus the mass number of projectile A_p.

differences in k_1 and k_2 are mainly caused by different data used.

In the table it is also shown that the mean HPF multiplicity $\langle n_\alpha \rangle$ is independent of the incident beam energy for the same projectile. The value of the dispersion of the HPF multiplicity distribution defined as $D = (\langle n_\alpha^2 \rangle - \langle n_\alpha \rangle^2)^{1/2}$ is also presented in the table. The variation of dispersion with mean HPF multiplicity is shown in Fig.4. The experimental points can be fitted by using a straight line in the form of $D = (-0.138 \pm 0.094) + (0.630 \pm 0.042)\langle n_\alpha \rangle$ and the χ^2/DOF=0.015. Sengupta *et al* [5] also have studied the same dependence by using the data from ^{16}O–, ^{32}S–, ^{56}Fe–, and ^{84}Kr–emulsion interactions, and they have observed the same tendency.

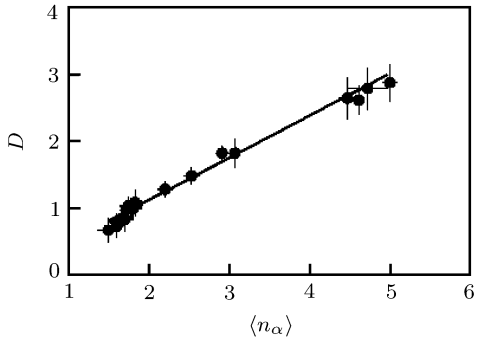


Fig.4. The dispersion of HPF multiplicity distribution versus $\langle n_\alpha \rangle$.

Table 1. Average HPF multiplicity $\langle n_\alpha \rangle$, moment C_q, dispersion D and the second Mueller moment f_2.

Projectile	$\langle n_\alpha \rangle$	C_2	C_3	C_4	C_5	D	f_2	Ref.
3.7 A GeV ^{12}C	1.49±.13	1.20±.10	1.71±.15	2.72±0.23	4.68±0.40	0.67±.18	–1.05±0.23	[13]
3.7 A GeV ^{16}O	1.60±.05	1.23±.07	1.81±.16	2.99±0.35	5.38±0.78	0.77±.12	–1.01±0.18	[12]
14.6 A GeV ^{16}O	1.7±0.1	1.2±0.1	1.7±0.1	2.6±0.2	4.3±0.1	0.76±.20	–1.12±0.29	[4]
60 A GeV ^{16}O	1.6±0.1	1.2±0.1	1.8±0.1	2.9±0.2	4.9±0.3	0.72±.18	–1.09±0.26	[3]
60 A GeV ^{16}O	1.62±.10	1.23±.07	1.77±.11	2.85±0.17	4.88±0.29	0.78±.13	–1.02±0.19	[5]
60 A GeV ^{16}O	1.7±0.1	1.2±0.1	1.7±0.1	2.8±0.1	4.7±0.2	0.76±.20	–1.12±0.29	[4]
60 A GeV ^{16}O	1.59±.03	1.21±.10	1.74±.10	2.82±0.10	4.96±0.20	0.73±.17	–1.06±0.25	[14]
200 A GeV ^{16}O	1.7±0.1	1.2±0.1	1.7±0.1	2.6±0.1	4.3±0.2	0.76±.20	–1.12±0.29	[4]
200 A GeV ^{16}O	1.60±.15	1.22±.11	1.74±.16	2.76±0.26	4.64±0.43	0.75±.20	–1.04±0.29	[5]
3.7 A GeV ^{20}Ne	1.60±.03	1.29±.03	2.09±.05	3.99±0.09	8.47±0.18	0.86±.05	–0.86±0.08	[13]
3.7 A GeV ^{24}Mg	1.71±.04	1.32±.03	2.24±.06	4.50±0.11	10.11±0.25	0.97±.05	–0.77±0.09	[3]
3.7 A GeV ^{24}Mg	1.71±.04	1.32±.10	2.24±.26	4.51±0.69	10.16±1.93	0.97±.15	–0.77±0.29	[1]
3.7 A GeV ^{24}Mg	1.8±0.1	1.3±0.1	2.1±0.1	3.9±0.2	7.9±0.5	0.99±.17	–0.83±0.32	[4]
3.7 A GeV ^{28}Si	1.79±.03	1.31±.06	2.14±.17	4.19±0.46	9.33±1.37	1.00±.10	–0.80±0.19	[16]
3.7 A GeV ^{28}Si	1.85±.07	1.32±.05	2.19±.08	4.35±0.16	9.87±0.25	1.05±.09	–0.75±0.17	[13]
14.5 A GeV ^{28}Si	1.78±.08	1.30±.06	2.11±.09	3.96±0.17	8.24±0.36	0.97±.11	–0.83±0.19	[7]
14.6 A GeV ^{28}Si	1.78±.05	1.34±.10	2.29±.27	4.65±0.73	10.58±2.09	1.04±.16	–0.70±0.31	[16]
14.6 A GeV ^{28}Si	1.7±0.1	1.3±0.1	2.3±0.1	4.6±0.2	10.6±0.5	0.93±.16	–0.83±0.29	[4]
200 A GeV ^{32}S	1.8±0.1	1.3±0.1	2.4±0.1	5.0±0.3	11.9±0.6	0.99±.17	–0.83±0.32	[4]
200 A GeV ^{32}S	1.7±0.1	1.3±0.1	2.3±0.1	4.7±0.2	11.0±0.4	0.93±.16	–0.83±0.29	[4]
200 A GeV ^{32}S	1.83±.06	1.35±.13	2.35±.35	4.95±1.04	11.90±3.36	1.08±.20	–0.66±0.44	[16]
200 A GeV ^{32}S	1.74±.10	1.35±.08	2.36±.13	5.03±.28	12.19±0.68	1.03±.13	–0.68±0.24	[5]
1.9 A GeV ^{40}Ar	2.20±.09	1.34±.06	2.19±.10			1.28±.12	–0.55±0.29	[7]
1.9 A GeV ^{56}Fe	2.53±.09	1.34±.05	2.21±.08	4.31±0.16	9.57±0.35	1.48±.12	–0.35±0.33	[5]
1.5 A GeV ^{84}Kr	2.91±.08	1.39±.04	2.40±.07	4.87±0.14	11.14±0.32	1.82±.11	0.39±0.35	[5]
1.8 A GeV ^{84}Kr	3.07±.03	1.35±.08	2.23±.22	4.29±0.60	9.24±1.73	1.82±.21	0.23±0.75	Ours
10.6 A GeV ^{197}Au	4.61±.07	1.32±.05	2.08±.12	3.71±0.29	7.21±0.70	2.61±.21	2.19±1.07	Ours
10.6 A GeV ^{197}Au	4.72±.24	1.35±.07	2.21±.11	4.13±0.21	8.58±0.44	2.79±.31	3.08±1.65	[3]
10.6 A GeV ^{197}Au	5.00±.09	1.33±.06	2.11±.15	3.77±0.36	7.29±0.88	2.87±.27	3.25±1.51	[18]
160 A GeV ^{208}Pb	4.47±.10	1.35±.08	2.21±.20	4.11±0.49	8.40±1.30	2.64±.31	2.52±1.61	[2]

Finally, we discuss the second Mueller moment[22] $f_2 = \langle n_\alpha^2 \rangle - \langle n_\alpha \rangle(1 + \langle n_\alpha \rangle) = D^2 - \langle n_\alpha \rangle$ of the HPF multiplicity distribution. Mueller has shown that the binomial moment of multiplicity distribution is useful for describing and analysing multiparticle final states.

Assume the semi-inclusive hypothesis, $\langle n_\alpha^q \rangle = C_q \langle n_\alpha \rangle^q$, then the second Mueller moment will be written as

$$f_2 = -\langle n_\alpha\rangle[1-(C_2-1)\langle n_\alpha\rangle]. \quad (5)$$

A Poisson distribution has the property that f_q (f_2 and all higher-order correlation functions) is equal to zero. Conversely, if f_2 and higher moments of the distribution of final-state particles in a given reaction are zero, then the particles can be said to be produced independently in a classical sense. However, it can be shown that the conservation of momentum and the conservation of energy require some quantities in the f_q to be nonzero and in fact negative in a multiparticle production reaction. Further, the correlation function f_2 is the integral of the normalized two-particle density distribution or differential two-particle correlation function. That is, if $f_2 > 0$, then the particles tend to cluster compared with a classical random distribution. Conversely, if f_2 is negative, the particles are distributed more uniformly than a classical random distribution, or the distribution is narrower than Poisson's or the particles are anticorrelated. In Table 1 we present the results of the second Mueller moment of HPF multiplicity distribution for various projectiles, with nuclear emulsion collisions at different energies. The values of f_2 are calculated from the formula $f_2 = (C_2-1)\langle n_\alpha\rangle^2 - \langle n_\alpha\rangle$. The error of f_2 is calculated according to the general law of error propagation. It is shown that the f_2 moment is also independent of projectile energy for the same projectile, but it is dependent on the projectile mass number. For projectiles ^{12}C, ^{16}O, ^{20}Ne, ^{24}Mg, ^{28}Si, ^{32}S, ^{40}Ar, and ^{56}Fe the second Mueller moments are always negative, but for projectiles ^{84}Kr, ^{197}Au, and ^{208}Pb the values of f_2 are positive. Figure 5 shows the dependence of the second Mueller moment f_2 on the mean HPF multiplicity $\langle n_\alpha\rangle$. It can be seen that the second Mueller moment increases with the increase of $\langle n_\alpha\rangle$, but not linearly. The experimental data are fitted by using the following relation:

$$f_2 = -\langle n_\alpha\rangle(a + b\langle n_\alpha\rangle). \quad (6)$$

The best fitting parameters are $a = 1.192 \pm 0.121$ and $b = -0.407 \pm 0.062$, with χ^2/DOF=0.026.

Figure 6 shows the correlation between the second Mueller moment of HPF multiplicity distribution and the mass number of projectile. The experimental data from ^{12}C, ^{16}O, ^{20}Ne, ^{24}Mg, ^{28}Si, ^{40}Ar, ^{56}Fe and ^{84}Kr–emulsion collisions at a few GeV/nucleon (less than and equal to Dubna energy) can be well represented by a linear relation $f_2 = (-1.222 \pm 0.142) + (0.017 \pm 0.006)A_p$ with χ^2/DOF=0.010. For the data from various projectiles with emulsion interactions at different energies, the best fitting is $f_2 = (-1.251 \pm 0.116) + (0.018 \pm 0.004)A_p$ with χ^2/DOF=0.008, which is almost the same as the ones given above and further confirms that the second Mueller moment is just dependent on the projectile mass number at high energies. The second Mueller moment of HPF multiplicity distribution increases linearly with the projectile mass number. From the simulations we know that the second Mueller moment of HPF multiplicity distribution becomes zero at $A_p \approx 69$. For $A_p < 69$, $f_2 < 0$, which means that the HPF distribution is narrower than Poisson's or HPFs are anticorrelated, but for $A_p > 69$, $f_2 > 0$, which means that the HPF distribution tends to cluster compared with a classical random distribution, or the emission of HPFs is correlated. The relevant physical essence is not clear yet, but positive value of f_2 may be an indicator of helium cluster existing in the heavy nucleus.

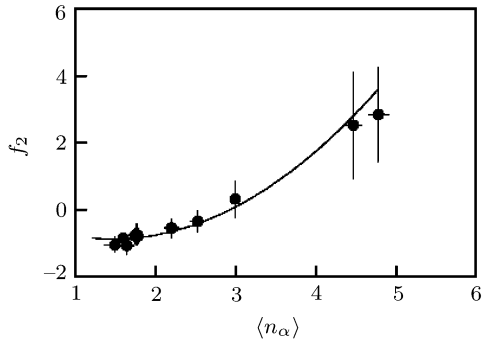


Fig.5. The second Mueller moment f_2 of HPF multiplicity distribution versus $\langle n_\alpha\rangle$.

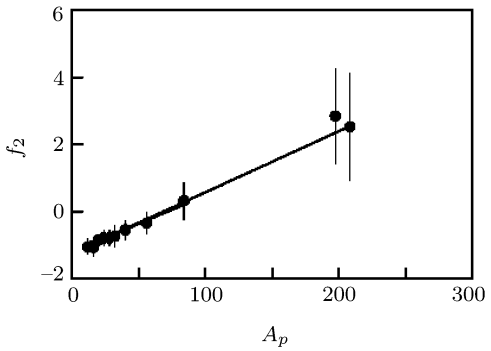


Fig.6. The second Mueller moment f_2 of HPF multiplicity distribution versus the mass number of projectile, A_p.

4. Conclusions

From the study of producing HPFs in relativistic nucleus–nucleus interactions, we can conclude that

the normalized multiplicity distribution of HPFs becomes broader with the increase of projectile mass number, which means that the average multiplicity of HPFs increases with the projectile mass number increasing. The HPF multiplicity distribution can be well described by using the KNO scaling presentation. Furthermore, the dispersion of HPF multiplicity distribution increases linearly with the mean HPF multiplicity. Finally, the second Mueller moment of the HPF multiplicity distribution also increases with the increase of the mean HPF multiplicity, or increases linearly with the projectile mass number, and the values of the second Mueller moment change from negative to positive with the increases of projectile mass number.

Acknowledgment

We are grateful to Professor I. Otterlund of the Lund University in Sweden for supplying the emulsion plates.

References

[1] Jilany M A 2004 *Phys. Rev.* C **70** 014901
[2] Singh G and Jain P L 1996 *Phys. Rev.* C **54** 3185
[3] Jilany M A 2004 *Eur. Phys. J.* A **22** 471
[4] El-Nadi M, El-Nagdy M S, Ali-Mossa N, Abdelsalam A, Abdalla A M and Abdel-Halim S M 2002 *J. Phys.* G **28** 1251
[5] Sengupta K, Singh G and Jain P L 1989 *Phys. Lett.* B **222** 301
[6] Adamovich M, Aggarwal M M, Arora R, Alexandrov Y A, Asimov S A, Basova E, Bhalla K B, Bhasin A, Bhatia V S, Bondarenkov R A, Burnett T H, Cai X, Chernova L P, Chernyavsky M M, Dressel B, Friedlander E M, Gadzhieva S I, Ganssauge E R, Garpman S, Gerassimov S G, Gill A, Grote J, Gulamov K G, Gulyamov U G, Hackel S, Heckman H H, Jakobsson B, Judek B, Kachroo S, Kadyrov F G, Kallies H, Karlsson L, Kaul G L, Kaur M, Kharlamov S P, Kumar V, Lal P, Larionova V G, Lindstrom P J, Liu L S, Lokanathan S, Lord J J, Lukicheva N S, Mangotra L K, Maslennikova N V, Mittra I S, Monnand E, Mookerjee S, Mueller C, Nasyrov S H, Navotny W S, Orlova G I, Otterlund I, Palsania H S, Peresadko N G, Persson S, Petrov N V, Qian W Y, Raniwala R, Raniwala S, Rao N K, Rhee J T, Saidkhanov N, Salmanova N G, Schulz W, Schussler F, Shukla V S, Skelding D, Soderstrom K, Stenlund E, Storey R S, Sun J F, Svechnikova L N, Tretyakova M I, Trofimova T P, Wang H Q, Weng Z Q, Wilkes R J, Xu G F, Zhang D H, Zheng P Y, Zhou D C and Zhou J C 1989 *Phys. Rev.* C **40** 66
[7] Singh G, Ismail A Z M and Jain P L 1991 *Phys. Rev.* C **43** 2417
[8] Jain P L and Aggarwal M M 1986 *Phys. Rev.* C **33** 1790
[9] Kamel K 1999 *Nuovo Cimento* A **112** 733
[10] Aggarwal M M, Bhalla K B, Das G and Jain P L 1983 *Phys. Rev.* C **27** 640
[11] Bahk S Y, Chang S D, Cheon B G, Cho J H, Jang H I, Hahn C H, Hara T, Lim G Y, Kang J S, Kim C O, Kim J Y, Kim K Y, Kim S N, Kim T I, Kim T Y, Koo D G, Lee S B, Lim I T, Moon K H, Nam S W, Pac M Y, Park I G, Park J N, Ryu J Y, Shin T S, Sim K S, Song J S, Woo J K, Yokoyama C and Yoon C S 1991 *Phys. Rev.* C **43** 1410
[12] Zhang D H, Li Z Y, Li J S and Wu F J 2004 *Chin. Phys.* **13** 1239
[13] El-Nadi M, Sherif M M, Abdelsalam A, Yasin M N, Bakr A, El-Nagdy M S and Jilany M A 1993 *Int. J. Mod. Phys.* E **2** 381
[14] Zhang D H 2002 *High Energy Phys. and Nucl. Phys.* **26** 40 (in Chinese)
[15] Singh G, Sengupta K and Jain P L 1990 *Phys. Rev.* C **42** 1757
[16] Adamovich M I, Aggarwal M M, Alexandrov Y A, Amirikas R, Andreeva N P, Anzon Z V, Arora R, Avetyan F A, Badayal S K, Bakich A M, Basova E S, Bazarov I K, Bhalla K B, Bhasin A, Bhatia V S, Bogdanov V G, Bradnova V, Bubnov V I, Burnett T H, Cai X, Carshiev D A, Chasnikov I Y, Chernova L P, Chernyavski M M, Dhamia S, Eligbaeva G Z, Eremenko L E, Gaitinov A S, Ganssauge E R, Garpman S, Gerassimov S G, Graf C, Grote J, Gulamov K G, Gupta S K, Gupta V K, Jakobsson B, Just L, Kachroo S, Kalyachkina G S, Kanygina E K, Karabova M, Kitroo S, Kharlamov S P, Kovalenko A D, Krasnov S A, Kumar V, Larionova V G, Li Y D, Liu L S, Lokanathan S, Lord J J, Lukicheva N S, Luo S B, Mangotra L K, Marutyan N A, Mashkov A Y, Maslennikova N V, Mittra I S, Mokerjee S, Nasyrov S Z, Navotny V S, Nystrand J, Ochs M, Orlova G I, Otterlund I, Peak L S, Peresadko N G, Petrov N V, Plyushchev V A, Qian W Y, Qin Y M, Raniwala R, Raniwala S, Rao N K, Roeper M, Rusakova G S, Shakhova C I, Shpilev S N, Skelding D, Soderstrom K, Solovieva Z I, Stenlund E, Svechnikova L N, Tothova M, Tretyakova M I, Trofimova T P, Tuleeva U I, Tursunov B P, Vokal S, Vrlakova J, Wang H Q, Weng Z Q, Wilkes R J, Xia Y L, Yang C B, Zhang D H, Zheng P Y, Zhokhova S I and Zhou D C 1995 *Z. Phys.* A **351** 311
[17] Singh B K, Ojha I D and Tuli S K 1994 *Nucl. Phys.* A **570** 819
[18] Singh G and Jain P L 1994 *Z. Phys.* A **348** 99
[19] El-Nadi M, Hussien A, Shaat E A, Abou-Moussa Z, Hamid A A and Kamel S 1995 *Nuovo Cimento* A **108** 935
[20] Koba Z, Nielsen D H and Olesen P 1972 *Nucl. Phys.* B **40** 317
[21] Song F and Zhang D H 2005 *Chin. Phys.* **14** 942
[22] Mueller A H 1971 *Phys. Rev.* D **4** 150